Consideration of recrystallization modeling of γ/γ'-strengthened Ni-based superalloys at sub-solvus temperatures

IOP Conf. Series: Journal of Physics: Conf. Series **1270** (2019) 012051 doi:10.1088/1742-6596/1270/1/012051

Consideration of recrystallization modeling of γ/γ′-strengthened Ni-based superalloys at sub-solvus temperatures

Takashi Nishimoto[1]*, Takuma Okajima[1], Qiaofu Zhang[2], Jiadong Gong[2]and Greg Olson[2]

[1] Corporate R&D Center, Daido Steel Co., Ltd., 2-30 Daido-cho, Minami-ku, Nagoya, Aichi, Japan

[2] QuesTek Innovations, 1820 Ridge Avenue; Evanston, IL, 60201, USA

* t-nishimoto@ac.daido.co.jp

Abstract. New Ni-based superalloys and methods for controlling their microstructures have recently received much investigation to further improve their high-temperature properties, sometimes via control of precipitates such as γ′ (Ni_3(Al,Ti,Nb,Ta)) and γ″ (Ni_3Nb). In Ni-based superalloys, fine grains favor deformability and mechanical properties; therefore, control of grain size, achieved by recrystallization, is also important. Some new studies have reported the pinning effects of coarse γ′. However, few studies have investigated modeling methods for recrystallization behaviors. Difficulties in grain size and phase distribution control have hindered fabrication by open-die forging utilizing the pinning effect of the γ′ phase. Therefore, this study examines the recrystallization behaviors of Ni-based superalloys containing coarse primary γ′ precipitates and considers applicable modeling methods. The recrystallization behaviors at sub-solvus temperatures are investigated in a new Ni-based superalloy with abundant coarse γ′ precipitates. Grain growth is limited by the pinning effect of coarse γ′ and the recrystallized grain size corresponds to increasing applied strain. Dynamic and static recrystallization is promoted by high strains and high temperatures. The kinetics of the recrystallized area fraction and recrystallization grain growth influenced by the pinning effect of coarse γ′ is modeled by Zurob's method.

1. Background

Ni-based superalloys have excellent high-temperature strengths. Recently, in order to further improve their high-temperature mechanical properties, the abundance of intermetallic compounds such as γ′ (Ni_3(Ti,Al,Nb,Ta)) and γ″ (Ni_3Nb) has been increased. However, control of grain size and precipitation morphology is also important in superalloys. Generally, Ni-based superalloys require fine grain structures to attain good hot workability [1] and high-temperature mechanical properties. Creep properties, which are of great importance, are enhanced by coarse grains; however, other properties such as fatigue properties, yield stress, and tensile stress are improved by fine grains. Therefore, obtaining structures with grains that promote both types of properties is necessary. Ni-based superalloys comprise only γ phases; refinement by phase transformation cannot be applied and recrystallization is the only method available for grain refinement. Therefore, microstructural control is achieved by hot rolling and hot forging. These refinement methods have received significant study. Grain refinement can be achieved by the pinning effects of precipitations such as carbides [2] and spheroidized δ phases [3]. A forging method applying the pinning effect of coarse primary γ′ was also reported recently [4-6]. Studies

have suggested that the recrystallization behaviors of precipitated coarse primary γ′ are very complex. The mechanism of recrystallization behavior has been extensively investigated.
Daido Steel Co. has developed the Daido Numerical Engineering System (DAINUS) to optimize the manufacturing process [7]. In previous studies, the manufacturing processes for Ni-based superalloys 706 and 718 have been optimized by applying DAINUS [8]. However, methods for modeling recrystallization behaviors with coarse primary γ′ have received little attention. Therefore, DAINUS cannot be directly used for microstructural predictions regarding coarse γ′. It is therefore difficult to optimize the manufacturing process of γ′-strengthened Ni-based superalloys with abundant γ′ precipitates. In this study, the recrystallization behaviors with precipitated coarse primary γ′ are investigated and modeling methods for this behavior are considered for microstructural predictions using DAINUS.

2. Experimental procedure

2.1. Materials and initial heat treatment

In order to investigate the recrystallization behaviors at sub-solvus temperatures, a new γ′-strengthened Ni-based superalloy Alloy A was used in this study. The chemical composition of Alloy A is shown in Table 1. The γ′-solvus temperature of Alloy A is measured by differential thermal analysis (DTA) as 1078 °C. Alloy A was melted by vacuum induction melting–electric slag remelting–vacuum arc remelting. Afterward, homogenization heat treatment and forging at super-solvus temperatures were performed. In order to precipitate coarse primary γ′, over-aging heat treatment was applied after forging. The average grain size after heat treatment is approximately 200 μm, with petal-shaped coarse primary γ′ precipitates. The average size of γ′ precipitates is approximately 1 μm.

Table 1. Chemical composition of Alloy A (mass %).

	Ni	Cr	Co	Mo	W	Al	Ti	Nb	C
Alloy A	Bal.	16.0	20.0	3.0	2.5	3.3	1.8	2.7	0.01

2.2. Experimental condition of recrystallization behavior

An investigation of the recrystallization behavior was performed by Rastegaev compression testing [9] and reheating. Figure. 1 shows the experimental heat pattern; the detailed conditions of the forging and reheating tests are shown in Tables 2 and 3, respectively. All experimental temperatures were below the γ′-solvus temperature of 1078 °C to check the recrystallization behavior of the precipitated coarse primary γ′. All specimens were cooled by water to freeze the microstructures. To observe the microstructures and coarse primary γ′, all specimens were etched observed by optical micrography and scanning electron microscopy (SEM). In order to observe optical micrograph, cupric chloride solution (50ml ethanol + 50ml HCl + 5g cupric chloride) is used. To observe γ’ phase, 10% nitric acid is used and electrolyzed at 0.6mA for 2seconds. To analyze the details of the recrystallization behavior, electron backscatter diffraction (EBSD) was used.

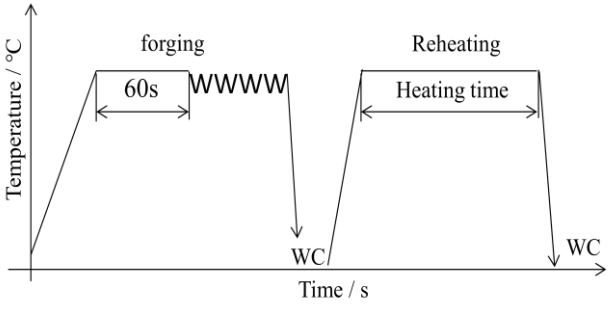

Figure 1. Heating applied for compression and reheating tests. WC: water cooling.

Table 2. Experimental Condition of compression test

Strain	0.2, 0.5, 0.8
Strain rate	0.5 s^{-1}
Forging temperature	1020, 1040 °C

Table 3. Experimental Condition of reheating test

Holding time	10800–72000 s
Heating temperature (Compression at 1020 °C)	1020, 1040, 1060 °C
Heating temperature (Compression at 1040 °C)	1040 °C

3. Experimental results

3.1. Microstructure as observed by optical micrography

Optical micrography results at the applied strains of 0.2 and 0.8 are shown in Figure 2. All microstructures follow the coarse prior γ grains; new recrystallized grains have originated from the previous grain boundaries. After reheating, the sizes of the prior γ grains are reduced to promote static recrystallization under all heating conditions. Recrystallization is promoted by the addition of high strains and heating at high temperatures for long periods. These results indicate features similar to those of the recrystallization of single-phase γ.After the reheating test, recrystallized grains grow from 10 to 20 μm. Compared with the grain growth behaviors of Waspaloy and Alloy 718 [10], grain growth is more restrained in Alloy A. One of the reasons for this behavior is the pinning effect of coarse primary γ′.

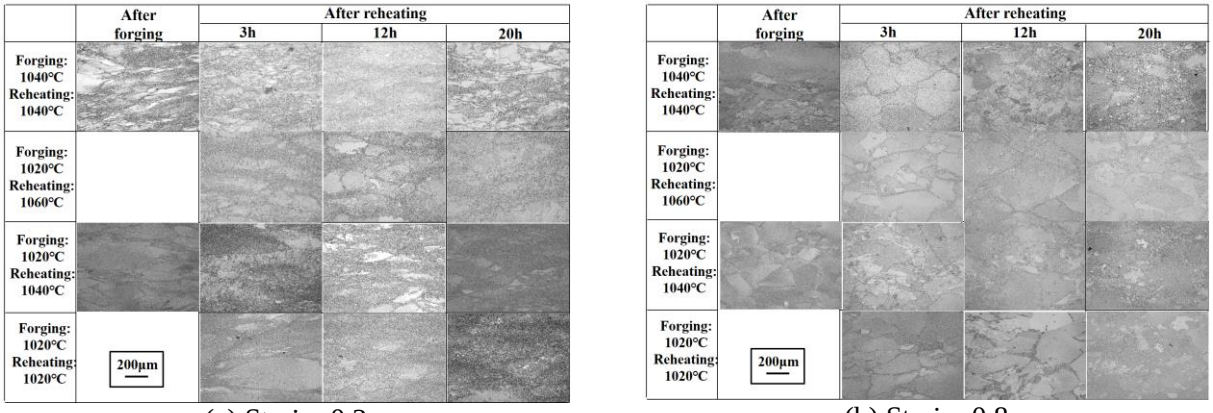

(a) Strain: 0.2 (b) Strain: 0.8

Figure 2. Optical micrograph after the experiments

3.2. Measurement results of coarse primary γ′

From the SEM images, the area fractions and diameters of coarse primary γ′ phases are measured by image analysis. The measured results at the strain level of 0.2 are shown in Figure 3. The area fractions of γ′ are increasing as the experimental temperature decreases. Compared to the results at different forging temperatures, the amount of γ′ differs. The amount of precipitated γ′ increases with increasing forging temperature. However, the amount of primary γ′ remains constant after reheating test. This indicates that the amount of coarse primary γ′ after reheating is less sensitive to the forging temperature. In addition, the reheating time has little influence on the amount of γ′.

Regarding the grain growth behavior of coarse primary γ′, the grain size is increased with increasing reheating temperature and reheating time.

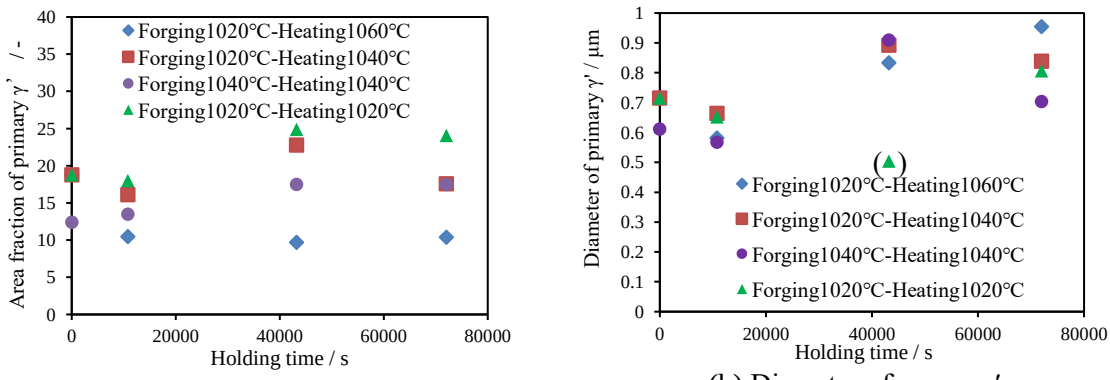

(a) Area fraction of coarse γ′ (b) Diameter of coarse γ′

Figure 3. Precipitation kinetics of gamma' phase at various temperature

3.3. Kernel average misorientation map analyzed by EBSD

In order to investigate the driving force of recrystallization, the dislocation density is measured by kernel average misorientation (KAM) analysis. KAM is a measurement of local orientation that relates to dislocation density. One report indicates that the dislocation density is correspondingly increased with increasing KAM values [11]. Figure 4 shows the KAM map obtained by EBSD at the strain of 0.2, as well as the relationship between temperature and holding time for the KAM values, which are defined by

$$K = \frac{\sum_{i=1}^{6n} \alpha_i}{6n}, \tag{1}$$

where K is the KAM value, n is the number of measurement points, and α_i is the misorientation angle. From the results of optical micrograph and KAM maps, the recrystallized grain area has generally low misorientation, while the high-misorientation areas do not experience recrystallization. Therefore, strain is recovered with grain recrystallization, while non-recrystallized grains restrain the dislocation density. In comparing the results after forging, the KAM value is increased with decreased forging temperatures. This indicates that the driving force for recrystallization corresponds with the forging temperature. After heating, the misorientation is reduced by strain recovery. The KAM values are decreased to a greater extent with higher-temperature and longer-duration heating.

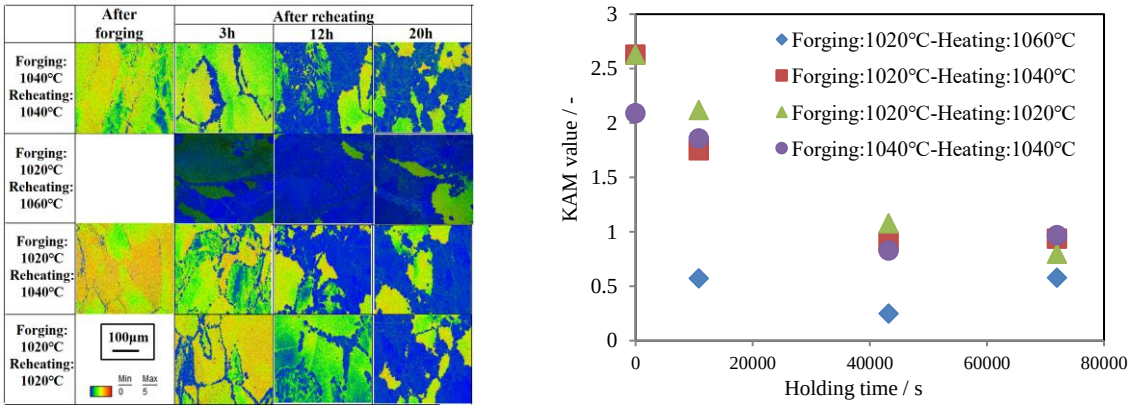

(a)Results of KAM map (b)Results of KAM value

Figure 4. Reslt of KAM maps from EBSD analysis after experiments

4. Consideration of modeling method of recrystallization behavior

4.1. Definition of static recrystallized area fraction

In order to consider modeling methods for this alloy at sub-solvus temperatures, the recrystallized area fraction and recrystallized grain size are measured by the grain size distribution results obtained via EBSD analysis. In this study, modeling methods for dynamic and static recrystallization are considered separately. For dynamic recrystallization, the recrystallized area fraction and grain sizes are measured using the forging test results. The grain size of static recrystallization is obtained using the reheating test results; the area fraction of static recrystallization is defined by:

$$X_{\mathrm{st}} = \frac{X_{\mathrm{total}} - X_{\mathrm{dyn}}}{1 - X_{\mathrm{dyn}}} \tag{2}$$

where X_{total} is the total area fraction of static and dynamic recrystallization from the reheating test results, X_{dyn} is the area fraction of dynamic recrystallization, and X_{st} is the area fraction of static recrystallization. X_{st} is calculated by equation (2).

4.2. Modeling of area fraction of dynamic recrystallization

Modeling of the dynamic recrystallization is considered using the X_{dyn} results. In this study, the area fraction of dynamic recrystallization is determined by equation (3):

$$X_{\mathrm{dyn}} = 1 - \exp\{-\ln 2 \times (\frac{\varepsilon}{\varepsilon_{0.5}})^n\} \quad (3)$$

where ε is the strain, $\varepsilon_{0.5}$ is the strain at which X_{dyn} is 0.5, and n is a coefficient. $\varepsilon_{0.5}$ is a function of temperature. A comparison of the measured and modeled results is shown in Figure 5. The modeled results have good precision compared to the measured results.

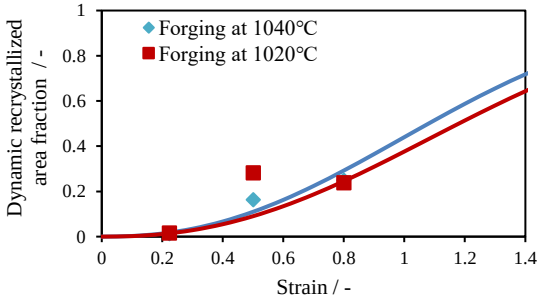

Figure 5. Modeling result of dynamic recrystallized area fraction.

4.3. Modeling of area fraction of static recrystallization

Modeling of static recrystallization is considered using the X_{st} results calculated by equation (2). Generally, the recrystallized area fraction is quantified by an Avrami-type equation:

$$X_{\mathrm{st}} = 1 - \exp\{-\ln 2 \times (\frac{t}{t_{0.5}})^n\} \quad (4)$$

where t is the holding time, $t_{0.5}$ is the time when X_{st} is 0.5, and n is a coefficient. However, in this case, it is difficult to apply because it does not consider the effect of driving force and pinning force. Therefore, the model reported by Zurob et al., which does consider these effects, is applied in this study [12]:

$$X_{\mathrm{st}} = 1 - \exp(-X_{\mathrm{ext}}) \quad (5)$$

$$X_{\mathrm{ext}} = \frac{A_0 \exp\left(\frac{Q}{RT}\right)}{RT} \int_0^t \left[B(\varepsilon) - 1.2 \frac{\gamma_{\mathrm{gb}} F_\gamma^{2/3}}{r} \right] \mathrm{d}t \quad (6)$$

where X_{ext} is the extended recrystallized fraction, Q is the activation energy, R is the gas coefficient, T is heating temperature, $B(\varepsilon)$ is the driving force of recrystallization, γ_{gb} is the grain-boundary energy of γ/γ', r is the radius of coarse primary γ', and F_γ is the area fraction of γ'. From the KAM map obtained after forging, the KAM increases with low-temperature forging, indicating that the driving force depends on the forging temperature. However, the gap in X_{st} for forging at different temperatures is slight. Therefore, $B(\varepsilon)$ is a function of strain in this study. F_v and r are obtained from the measurement results. The modeling results of static recrystallization are shown in Figure 6, which shows high strain. The precision of the modeling result increases with increasing strain.

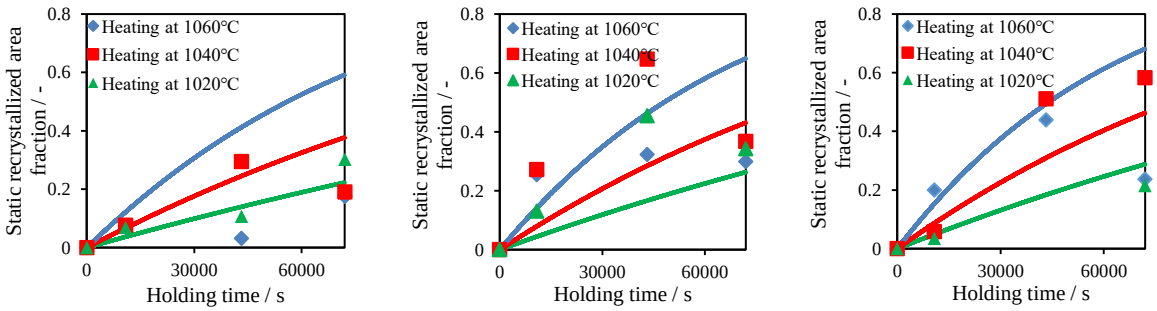

(a) Strain: 0.2 (b) Strain: 0.5 (c) Strain: 0.8

Figure 6. Static recrystallization modeling result of Alloy A

4.4. Modeling results for integrated dynamic and static recrystallization

The modeling results for integrated dynamic and static recrystallization are shown in Figure 7. The modeling results fit very well with the experimental results, especially at high-strain conditions. The pinning force for coarse primary γ′ and the driving force of recrystallization fluctuate continuously during forging and reheating. Therefore, microstructural prediction via the applied Avrami-type equation is difficult. A new modeling method for predicting the recrystallized area fraction is thus established by applying the modified model developed in this study.

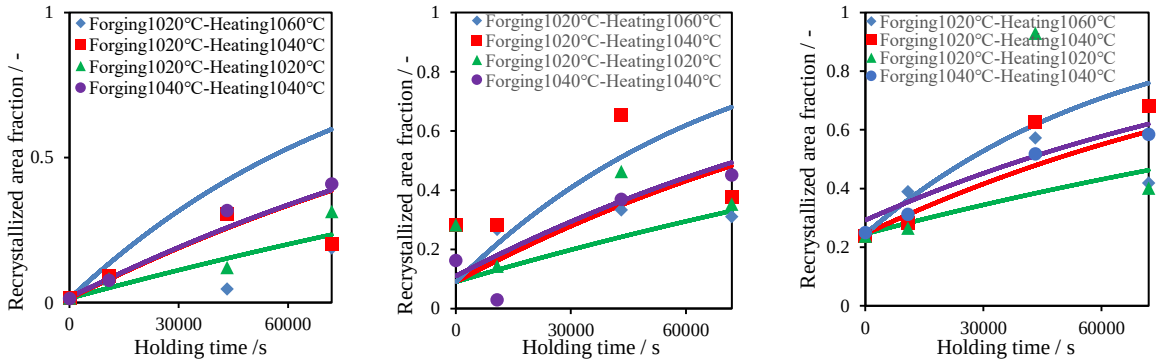

(a) Strain: 0.2 (b) Strain: 0.5 (c) Strain: 0.8

Figure 7. Recrystallization modeling result of Alloy A

5. Conclusion

(1) Recrystallization occurred in Alloy A from the grain boundaries of prior γ with coarse primary γ′. In addition, recrystallization is promoted by heating at high temperature, applying high strain, and maintaining heating for a long duration. Grain growth is restricted by the pinning effect of coarse γ′.

(2) The area fraction of coarse primary γ′ is changed by the heating temperature; the grain size of γ′ is increased with heating. The KAM value correspondingly increases with increases in the forging temperature. These trends indicate that the pinning force and driving force of recrystallization fluctuate continuously during forging and reheating.

(3) The microstructure is difficult to predict by applying Avrami-type equations because they cannot consider the fluctuation of these effects. The proposed modified model may accommodate these effects and shows good microstructural prediction for Alloy A with coarse primary γ′.

References

[1] Bi Z, Lv X and Zhang J 2014 *EUROSUPERALLOYS 2014 – 2nd European Symp. on Superalloys and their Applications* **14** 07002
[2] Ruan J J, Ueshima N and Oikawa K 2018 *J. Alloys Compd* **737** 83–91
[3] Masanuga A, Furuse T, Yoshida H, Okajima T, Hatta T and Isogawa S 2006 *IFM2006: 16th International Forgemasters Meeting* **16** p. 571
[4] Collins D M, Conduit B D, Stone H J, Hardy M C, Conduit G J and Mitchell R J 2013 *Acta Mater* **61** 3378.
[5] Charpagne M A, Billot T, Franchet J M and Bozzolo N (2016) *Superalloy2016 Proc.* p. 417.
[6] Thebault J, Solas D, Rey C, Baudin T, Fandeur O and Clavel M (2008) *Superalloys 2008 Proc.* p. 985
[7] Yoshida H, Hatta T, Hironaka T, Isogawa S and Sekiguchi H 2007 *NUMIFORM Proc.* p. 987
[8] Hatta T, Hironaka T, Yoshida H, Isogaiwa S and Sekiguchi H 2008 *Int. Conf. IFM2008* p. 472.
[9] P. Christiansen,P. A. F. Martins and N. Bay 2016 *Experimental Mechanism* 56 1271-1279
[10] Okajima T, Sakurai S, Fujiwara M 2014 *Int. Conf. IFM2014* p. 198.
[11] Umezaki S, Murata Y, Nomura K and Kubushiro K 2014, *J. Jpn. Inst. Met. Mater.* **78** 218–24
[12] Zurob H S, Hutchinson C R, Brechet Y and Purdy G 2002 *Acta Mater.* **50** 3075–92